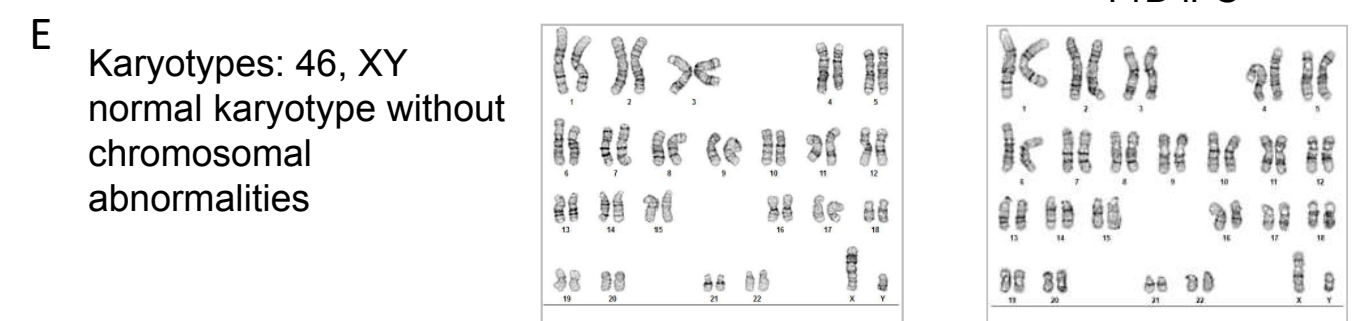
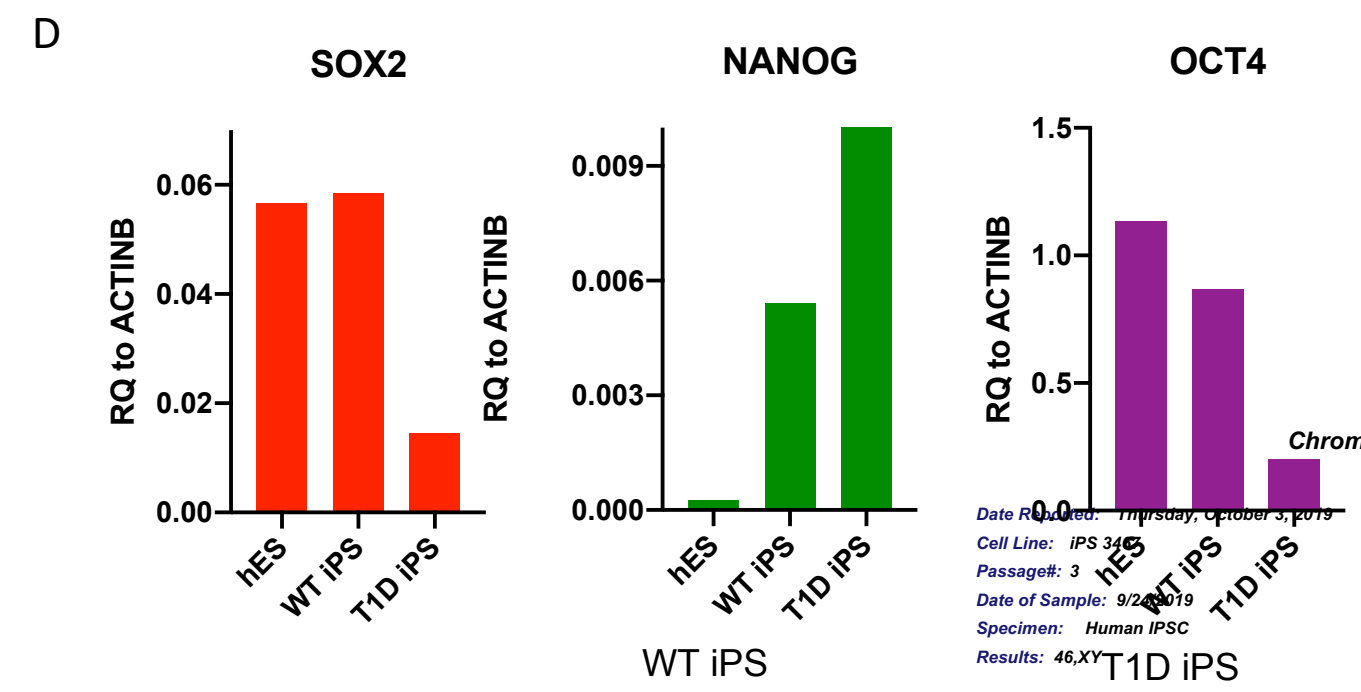
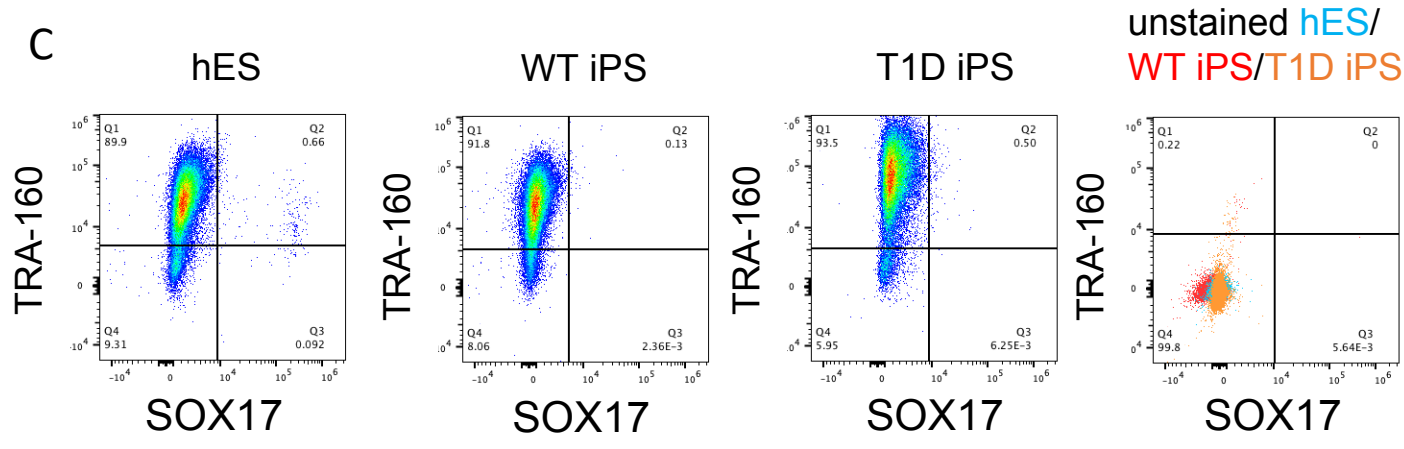
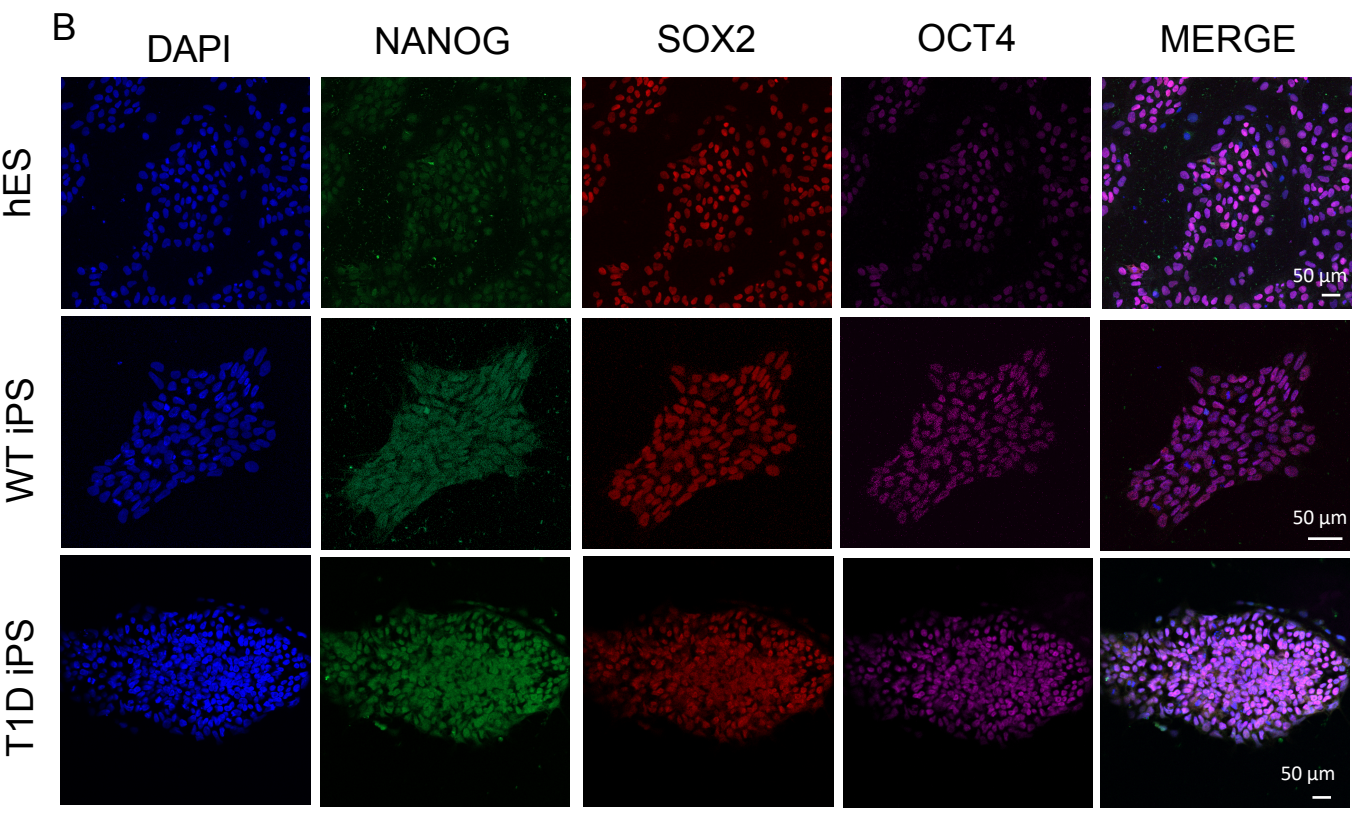
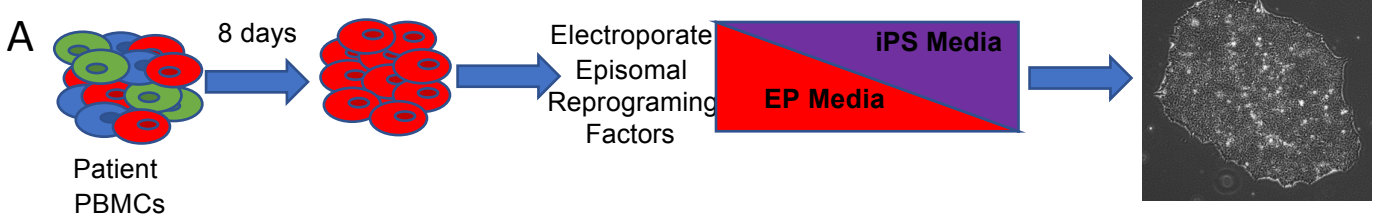


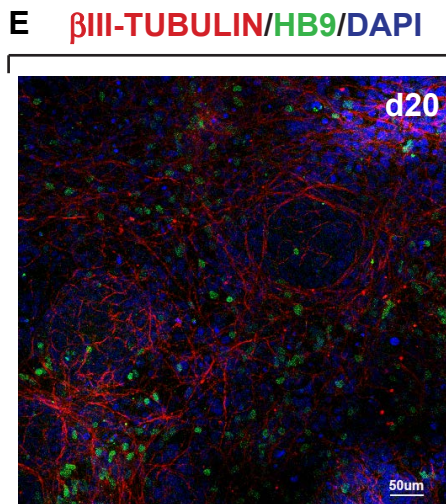
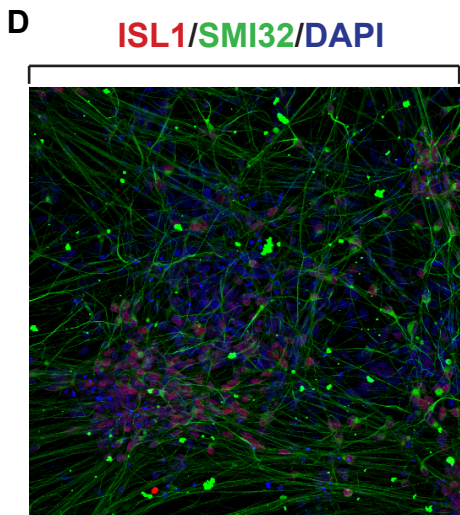
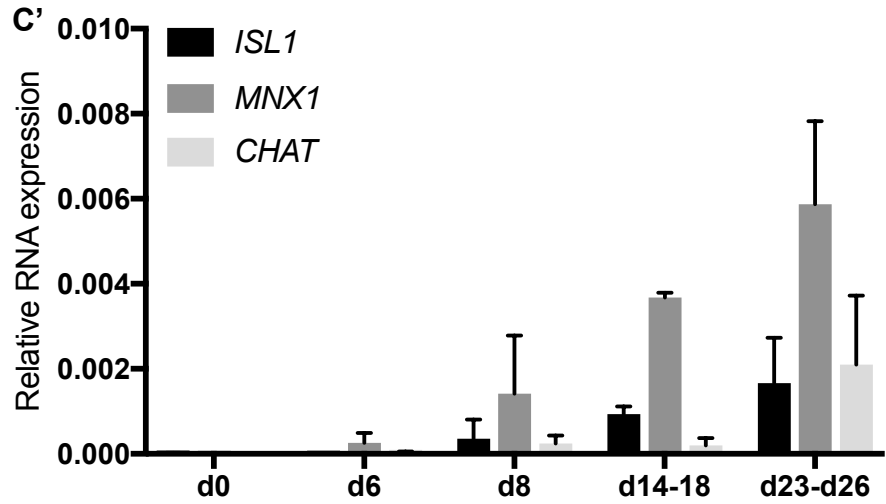
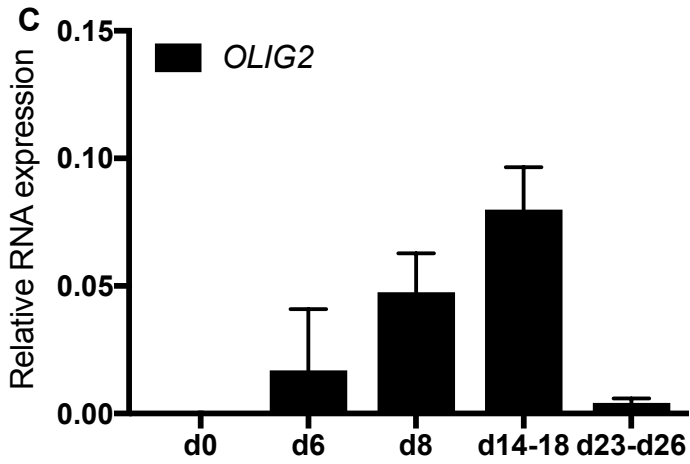
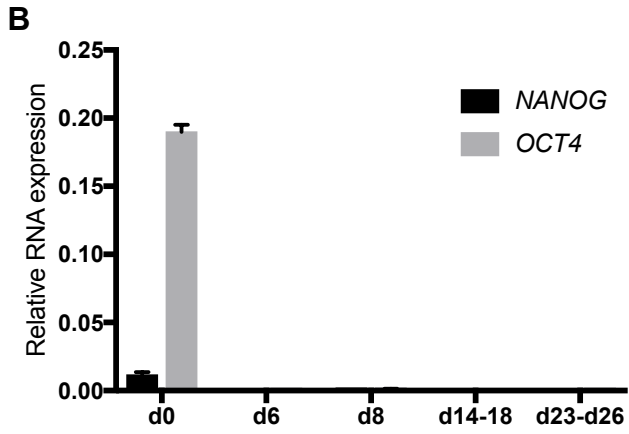
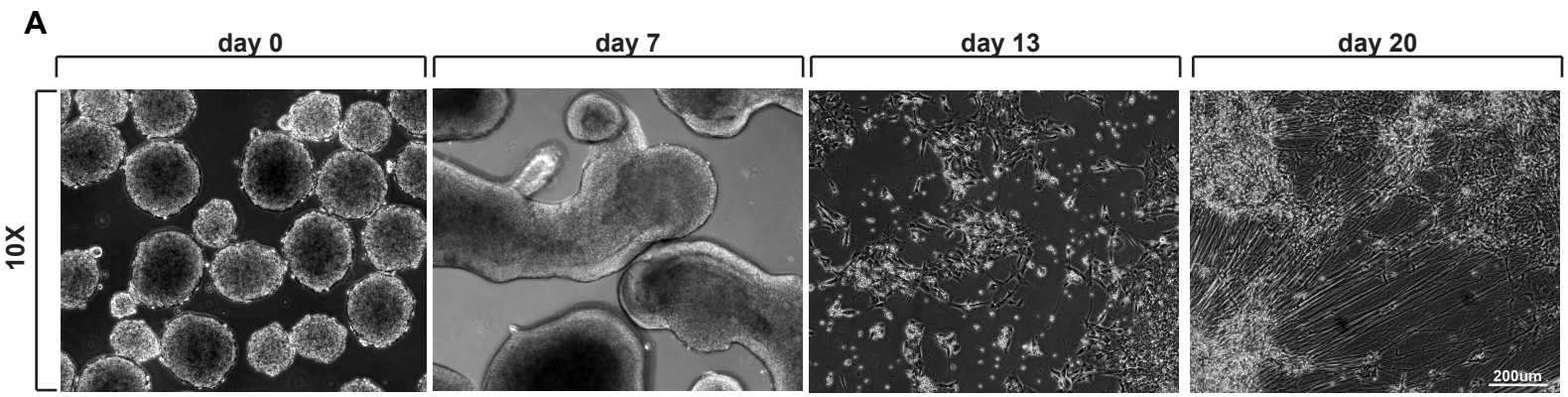
Stem Cell Reports, Volume 14

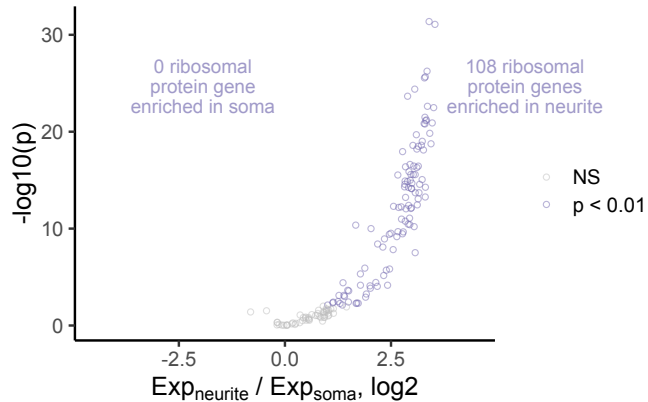
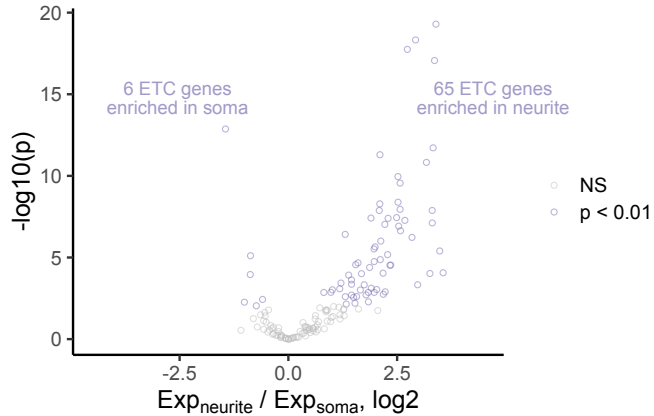
Supplemental Information

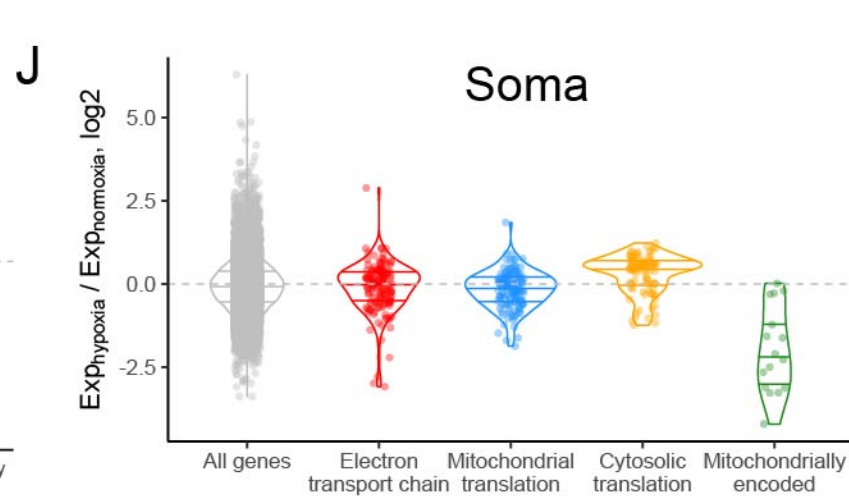
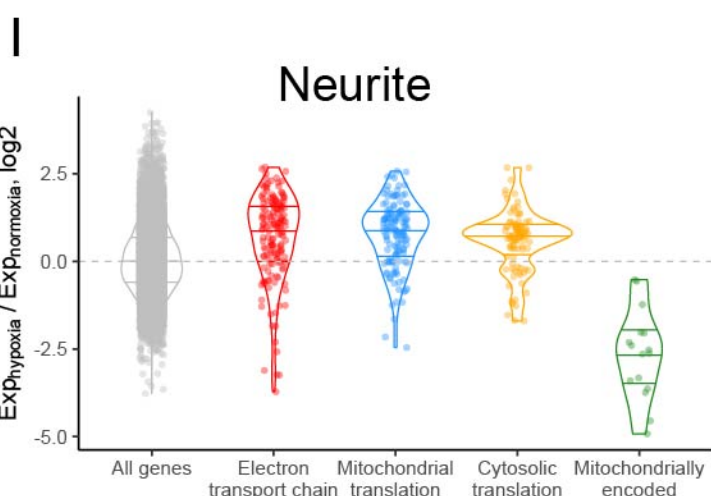
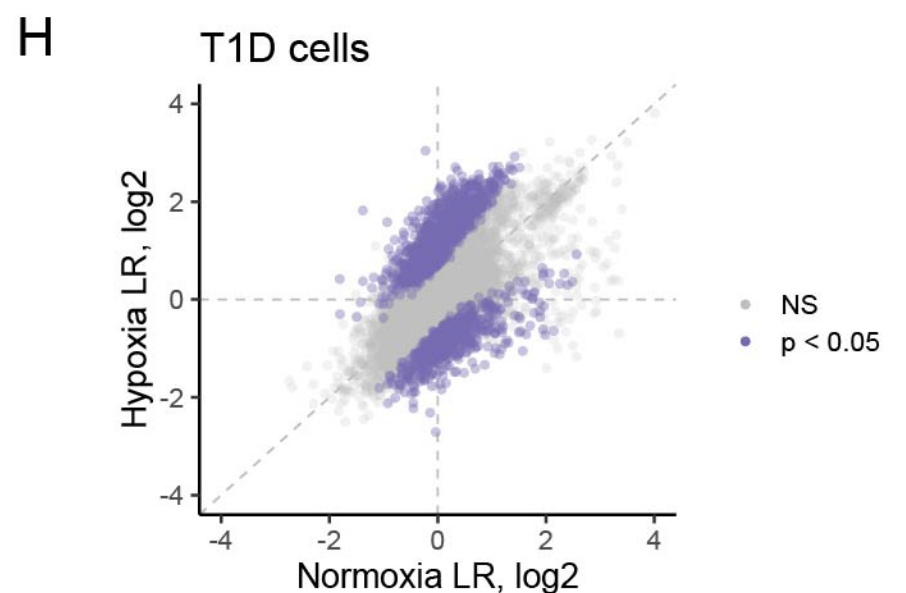
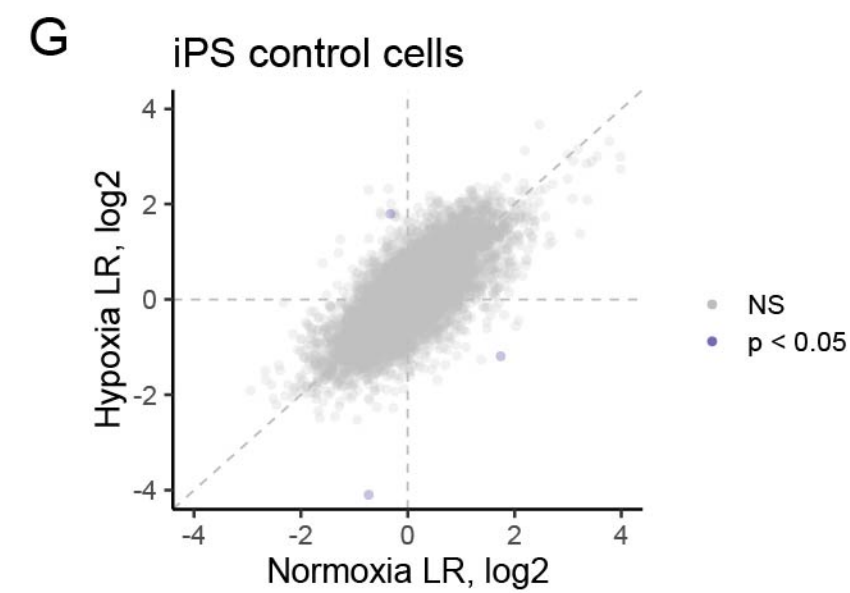
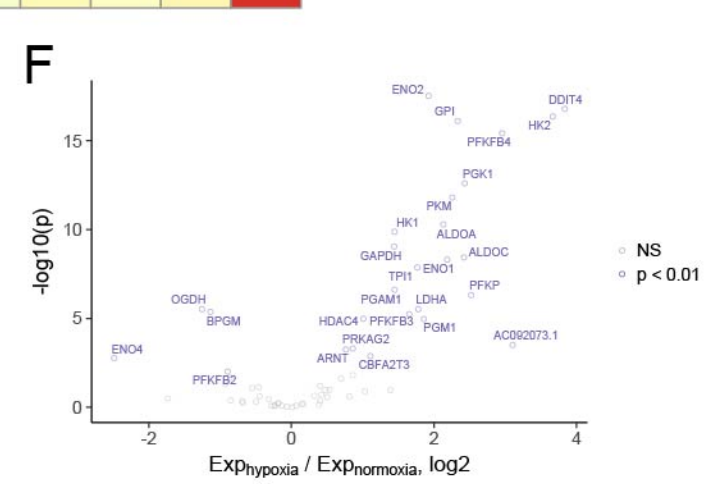
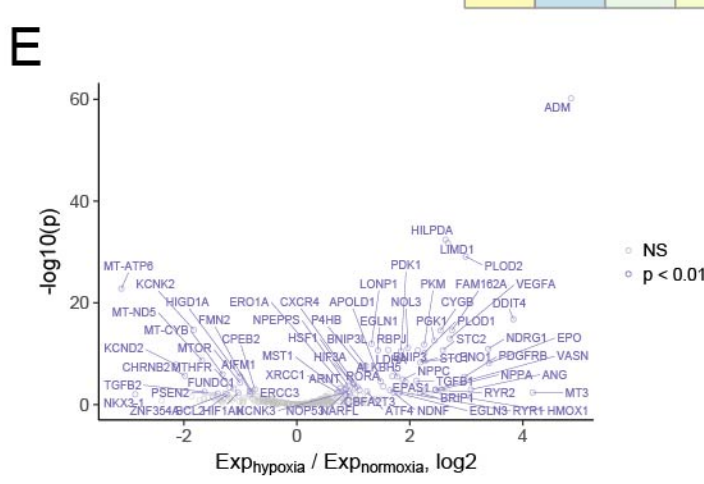
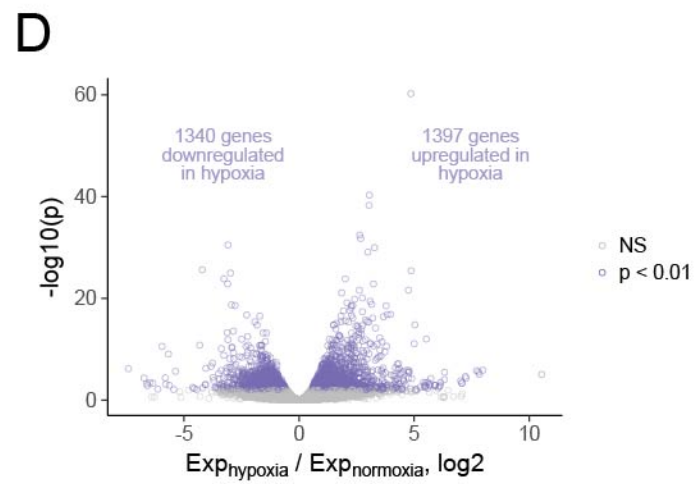
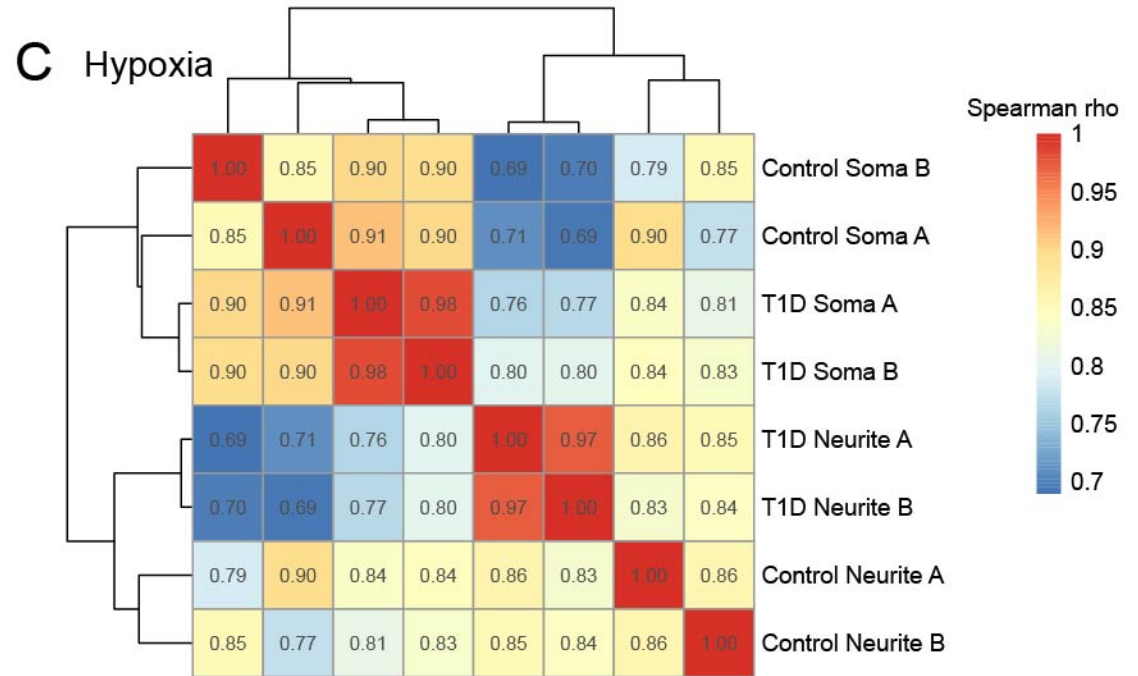
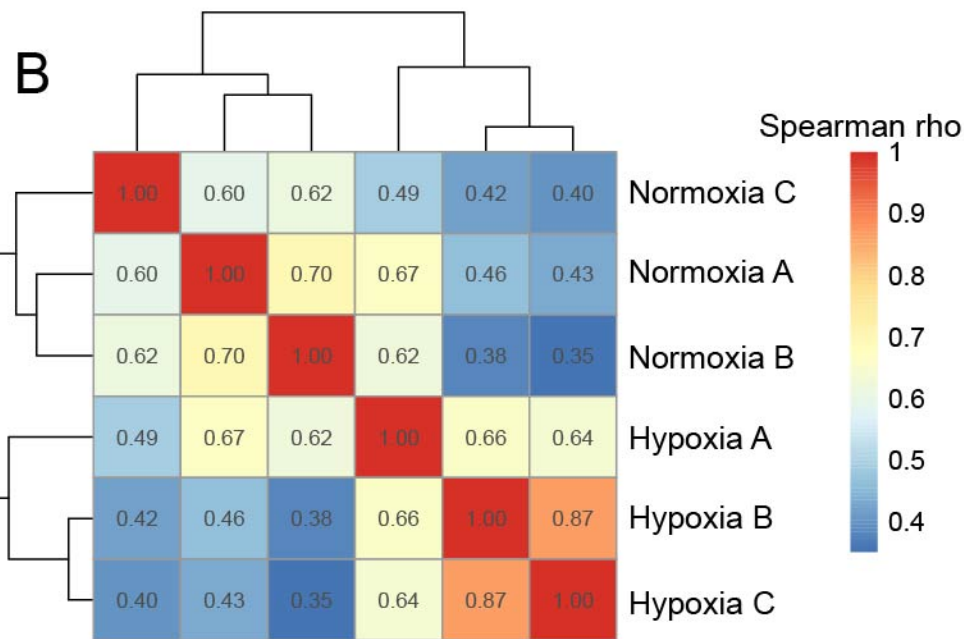
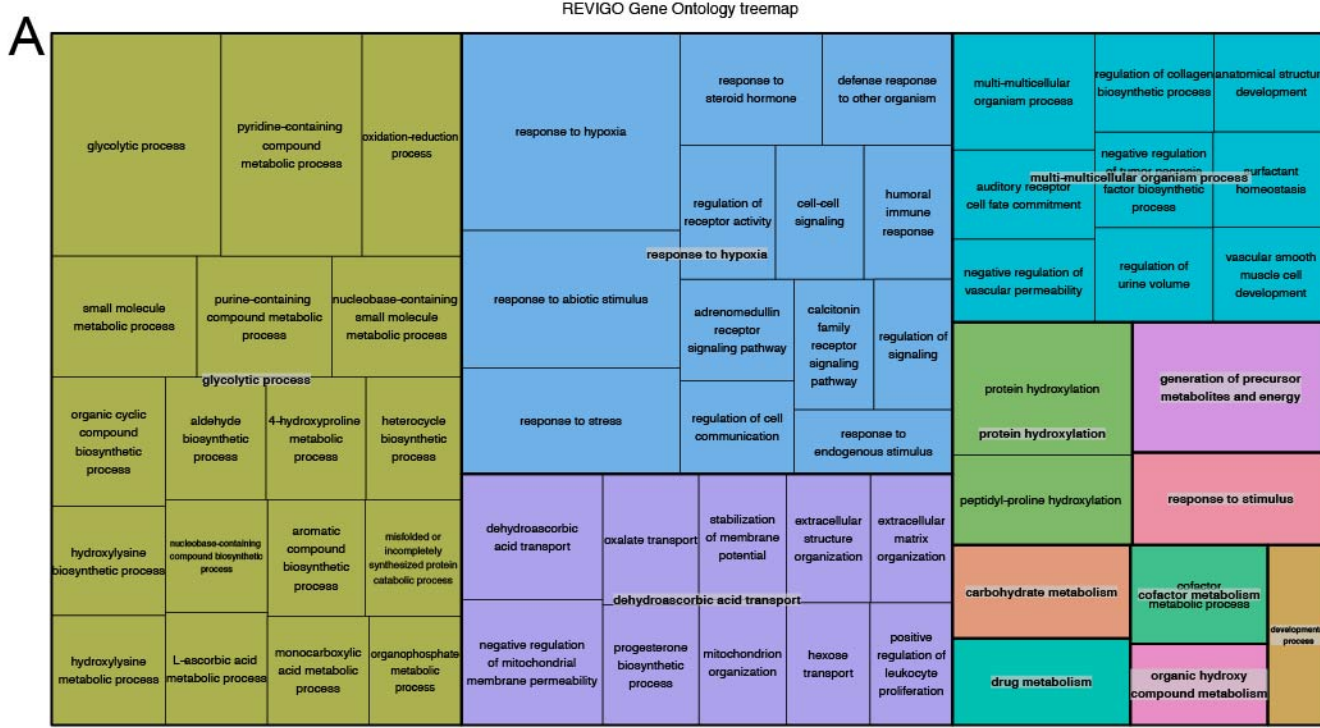
Modeling Hypoxia-Induced Neuropathies Using a Fast and Scalable Human Motor Neuron Differentiation System

Laura I. Hudish, Andrew Bubak, Taylor M. Triolo, Christy S. Niemeyer, Lori Sussel, Maria Nagel, J. Matthew Taliaferro, and Holger A. Russ





A**B**



Supplementary Figure 1: Generation of patient specific induced pluripotent stem cells (iPSCs). (A) Schematic outlining the reprogramming approach and micrograph of emerging clonal, patient specific iPSC colony. (B) Immunofluorescence analysis of pluripotency markers NANOG, OCT4 and SOX2 in established iPSC and control hESC cells. (C) Flow based quantitative analysis for the pluripotency marker TRA1-60 and the endodermal marker gene SOX17 in iPSC and control hESC. (D) qPCR analysis for pluripotency markers *NANOG*, *OCT4* and *SOX2* of iPSC and control hESC n=1-3 independent experiments. (E) Established iPSCs exhibit a normal karyotype as assayed by G-Band karyotyping.

Supplementary Figure 2. Suspension culture based direct differentiation approach of in-house reprogrammed, patient specific iPSCs into human motor neurons. (A) Representative images taken at the indicated magnification at key stages of the differentiation protocol. Scale bar = 200um. (B) Quantitative PCR analysis of pluripotency markers *NANOG* and *OCT4* normalized to *TBP* at subsequent stages of differentiation. n=2 independent experiments, data is presented as SEM. (C) Quantitative PCR reveals expression of MN progenitor marker *OLIG2* peaks at d14 and becomes significantly reduced by d23. (C') Mature MN markers *ISL1* and *MNX1* expression is detectable at d14 and is maintained at d23, at which point

CHAT expression also becomes highly enriched. n=2 independent experiments, data is presented as SEM. (D) Immuno-fluorescence analysis for neuronal markers of d20 MNs, Scale bar = 50um.

Supplemental Figure 3: Quality control of soma / neurite fractionation.

mRNAs that encode ribosomal proteins and components of the electron transport chain are enriched in neurites. (A) mRNAs that encode ribosomal proteins and electron transport chain components (B) are strongly enriched in neurite samples. Significantly enriched ($p < 0.01$, \log_2 fold change > 1.5) genes are in purple. Both of these categories have been repeatedly seen as neurite-enriched in previous neuron fractionation studies, demonstrating the validity of these fractionations and samples.

Supplemental Figure 4. Changes in gene expression in response to hypoxia.

Cellular responses to hypoxia at the level of RNA metabolism. (A) Gene ontology analysis of genes that were differentially expressed between normoxia and hypoxia conditions. Terms related to the response to hypoxia and glycolysis were the two most highly enriched categories. (B) Hierarchical clustering of LR values from normoxia and hypoxia- treated ES derived and (C) iPS control and T1D motor neurons. (D) LR values from normoxia and hypoxia-treated iPS control and (E) iPS T1D motor neurons. Genes with significant ($p < 0.05$) changes in LR between conditions are colored in purple. (F) Differentially expressed genes between normoxia and hypoxia samples. Significantly differentially genes ($p < 0.01$, \log_2 fold change > 1.5) are in purple. (G) Differentially expressed genes that contain the GO term “response to hypoxia”. (H) Differentially expressed genes that contain the GO term “glycolytic process”. (I, J) Gene expression differences between normoxia and hypoxia conditions in neurite (I) and soma (J) samples. In neurite samples, genes involved in the electron transport chain and mitochondrial translation are more expressed in hypoxia conditions relative to normoxia. However, in soma samples, there is no difference in expression. Genes involved in cytosolic translation are upregulated in response to hypoxia in both neurite and soma compartments. Mitochondrially-encoded genes are downregulated in both compartments, but the level of downregulation is greater in neurite than in soma.

Supplemental Table 4

Reagent	Company	Cat#	Final Concentration
Knock Out DMEM F12	Gibco	12660012	
Glutamax	Gibco	35050061	1X
2-Phospho-L-Ascorbic Acid	SIGMA-ALDRICH	49752	50mM
N2 Supplement A	Stemcell technologies	7152	1X
SM1 supplement	Stemcell technologies	5710	1X
SAG	Stemcell technologies	73412	200nM
Dorsomorphin (Compound C)	Stemcell technologies	72102	1uM
TTNPB	Stemcell technologies	72892	1.5uM
BDNF	Stemcell technologies	78005	0.02ug/mL
GDNF	Stemcell technologies	78058	0.02ug/mL
CHIR99021	Stemcell technologies	72052	4uM
SB431542	Stemcell technologies	72232	10uM
γ-Secretase Inhibitor XX	Calbiochem	565789	2uM
Rock Y-27632	Selleck Chemical LLC	S1049	5uM

SYBR PRIMERS		
Gene	Forward	Reverse
hTBP	CCTGCCGATAACTATCTCTGGC	GTTTCCACGGATGCTTTCTCG
hHOXA1	AAATCAGGACCACACAGAC	GTAGCCCTCTCCAAC TTTC
hHOXB3	GGCAAACGTCCAAGCTGAA	CTCCAGCTCCACCAGCTGCG
hHOXC4	GAGAGAGGTAGTGAGCGTCC	CTGGCCCAGCTTTTCACAAT
hHOXC5	ACAGATTTACCCGTGGATGAC	AGTGAGGTAGCGGTTAAAGTG
hHOXC6	GAATGAGGGAAGACGAGAAAGAG	CATAGGCGGTGGAATTGAGG
hHOXC8	TTTATGGGGCTCAGCAAGAGG	TCCACTTCCTTCGGTTCTG
hHOXC9	AGCACAAAGAGGAGAAGGC	CGTCTGGTACTTGGTGTAGG
hHOXB8	TAA GCG GCG AAT CGA GGT AT	TGT TTC TCC AGC TCC TCC TG
hHOXD8	CCT GAC TGT AAA TCG TCC AGT GGT A	AGT TTG GAA GCG ACT GTA GGT TTG
Taqman probe	Biorad FAM	
NANOG	CEP0050656	
OCT4	CEP0041056	
ISL1	CEP0049263	
OLIG2	CEP0025687	
MNX1	CEP0057720	
CHAT	CEP0049559	
TBP	CIP0036255	